Supplementary Material for

Simulation of adult limb regeneration with lizard tail spinal cord implants reveals distinct roles of radial glia and microglia populations.

Ricardo Londono, Zheyu Pan, Megan L Hudnall, Thomas P Lozito*

***Correspondence**: Thomas P Lozito
Email: lozito@usc.edu

This PDF file includes:

Supplementary Material Figure 1 - 16
Supplementary Material Table 1

Supplementary Figure 1. Quantified percentages of *ctsk*$^{+}$ tail and limb phagocytes within 500 µm of amputation planes that express microglia marker *sall1* 7 DPA. Tail phagocytes are subdivided ino spinal cord associated-phagocytes (defined as *ctsk*$^{+}$ cells within 150 µm of ependymal tubes) and "other" phagocytes more than 150 µm from ependymal tubes. Limbs do not naturally contain spinal cord tissue. n = 50 cell densities measured from five images among 10 different animals. Data are presented as mean values +/− SD. Two-way ANOVA with pairwise Tukey's multiple comparison tests was used. *, $p < 0.001$.

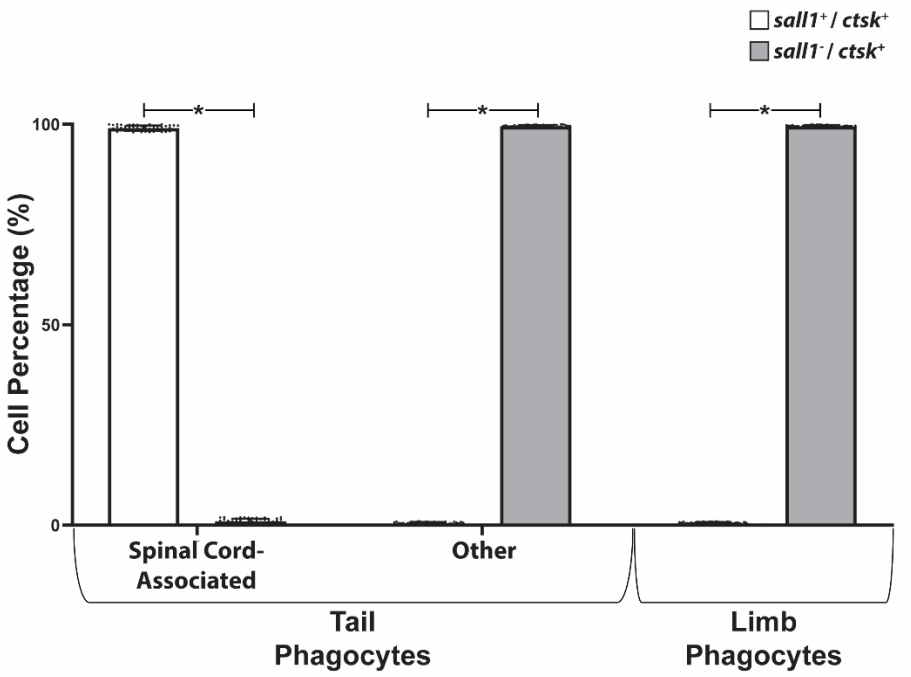

Supplementary Figure 2. RGC and microglia markers label distinct cell populations within regenerated lizard tail spinal cords. Representative transverse section of regenerated lizard tail (21 DPA) analyzed by histology/FISH for *sall1* and *fapb7* expression. *Fabp7*$^{+}$ RGCs are spatially distinct from *sall1*$^{+}$ microglia. et, ependymal tube; mg, microglia. Bar = 50 µm.

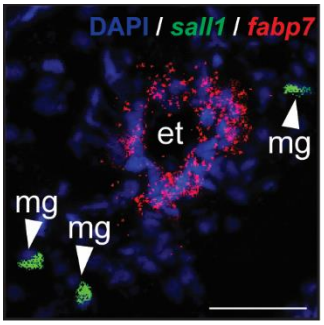

Supplementary Figure 3. Fluorescently labeled RGCs of original tail spinal cords contribute to regenerated tail ependymal tubes. (a) Experimental scheme for lineage tracing RGCs during lizard tail regeneration. RGCs within spinal cords of amputated original tail stumps were pre-labeled with AAV5 (GFAPp-Cre) and AAV5 (FLEX-DTR-GFP). Following 21 days of regrowth, regenerated tails were collected and analyzed for co-localization of GFP with expression of RGC marker *fabp7*. **(b)** Sagittal section of junction between original and regenerated tail regions of a lizard pre-treated with AAV5 (GFAPp-Cre / FLEX-DTR-GFP) analyzed by histology/FISH for GFP and *fabp7*. RGCs of both original tail spinal cords and regenerated tail ependymal tubes express GFP, indicting shared cell sources. et, ependymal tube; sc, spinal cord. Dashed line marks amputation plane. Bar = 100 µm.

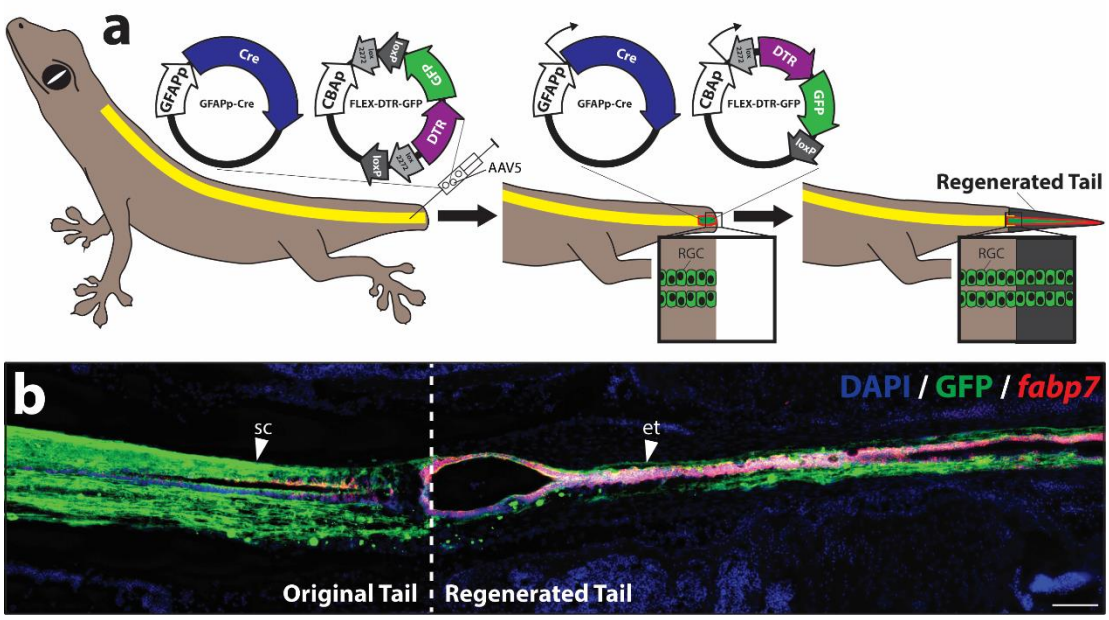

Supplementary Figure 4. Validation of targeted depletion of lizard spinal cord RGCs. Transverse sections of distal original tail samples collected from **(a-f)** Group 1, **(g-l)** Group 2, **(m-r)** Group 3, and **(s-x)** Group 4 lizards were analyzed by histology/FISH/fluorescence microscopy for GFP and DiI signals and for *fabp7* and *sall1* expression. Fluorescence channels are presented individually and merged to highlight colocalizations of markers. Arrow heads denote microglia. cc, central canal. Bar = 50 μm.

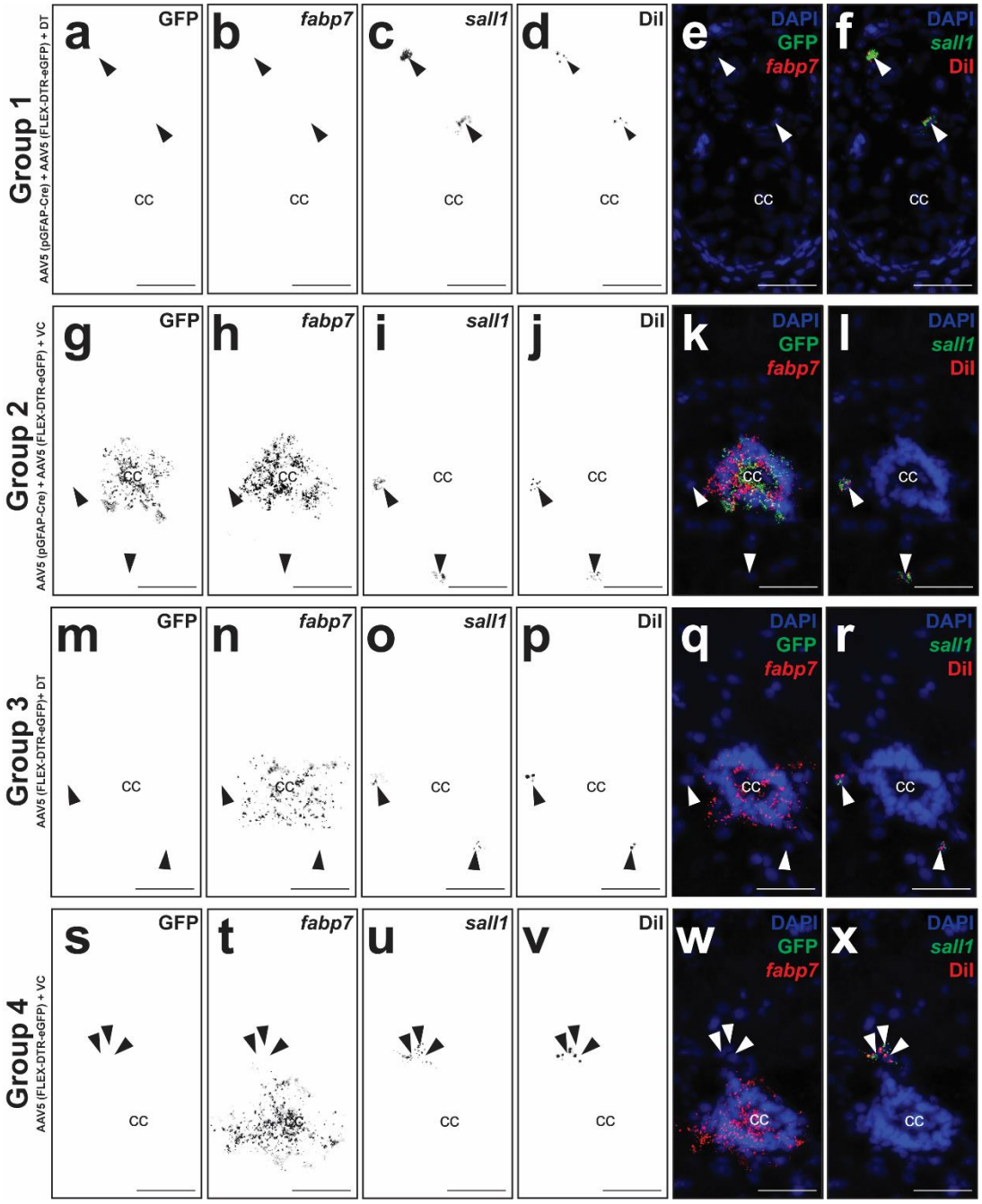

Supplementary Figure 5. (a, b) Gross morphology of representative tails collected 14 DPA from (a) Group 3 and (b) Group 4 lizards. **(c, d)** Sagittal sections of Group 3 and 4 lizard tails analyzed 14 DPA by fluorescence microscopy for EdU incorporation. Dashed lines mark amputation planes. **(e-h)** Higher magnification views of distal tail regions analyzed by histology/FISH for EdU incorporation and expression of *col3a1* and *acta2*. **(i)** Quantified percentages of *col3a1*$^{+}$ fibroblasts that exhibit EdU incorporation or express *acta2* among Group 3 and Group 4 samples. n = 10 different animals/tails for each condition. Data are presented as mean values +/− SD. Two-way ANOVA with pairwise Tukey's multiple comparison tests was used. ns, not significant compared to corresponding Group 2 values.

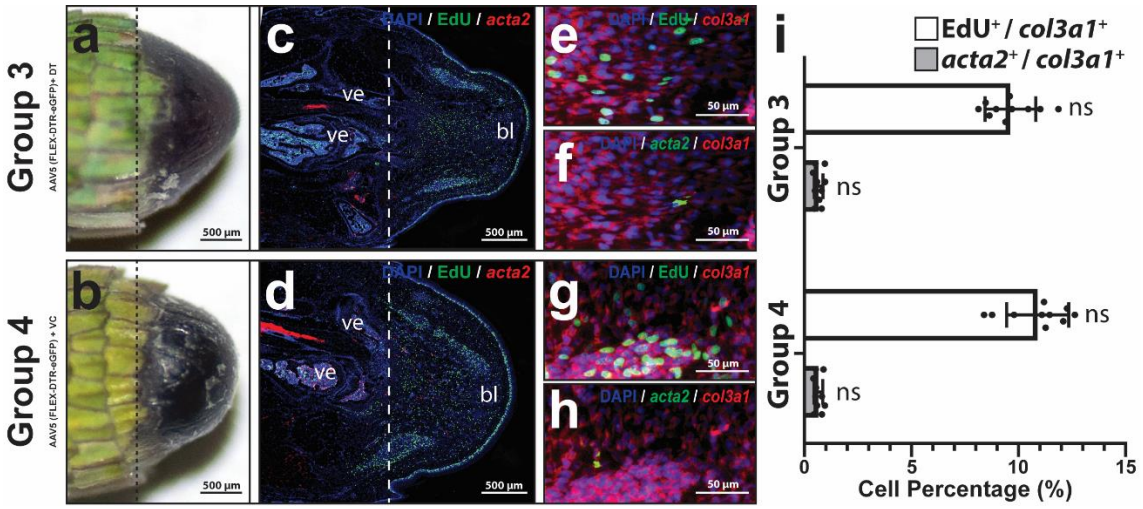

Supplementary Figure 6. Lengths and areas of tail tissues distal to amputation planes collected 14 DPA from lizards belonging to Groups 1, 2, 3, and 4. n = 10 different animals/tails for each condition. Data are presented as mean values +/− SD. Two-way ANOVA with pairwise Tukey's multiple comparison tests was used. *, #, &, $p<0.01$, compared to corresponding Group 2, 3, and 4 values, respectively.

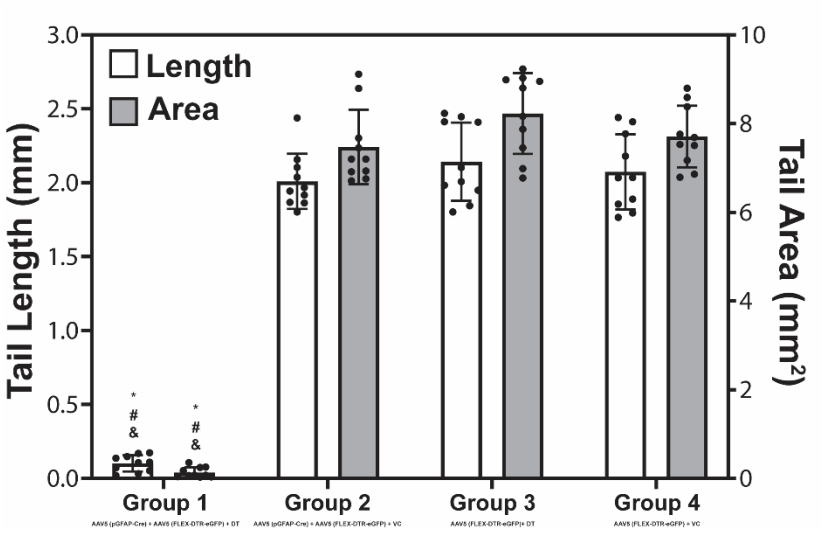

Supplementary Figure 7. Validation of targeted depletion of lizard spinal cord microglia. Transverse sections of distal original tail samples collected from lizards treated with **(a-e)** clodronate liposomes or **(f-j)** PBS liposomes were analyzed by histology/FISH/fluorescence microscopy for DiI signals and for *fabp7* and *sall1* expression. Fluorescence channels are presented individually and merged to highlight colocalizations of markers. Arrow heads denote microglia. cc, central canal. Bar = 50 µm.

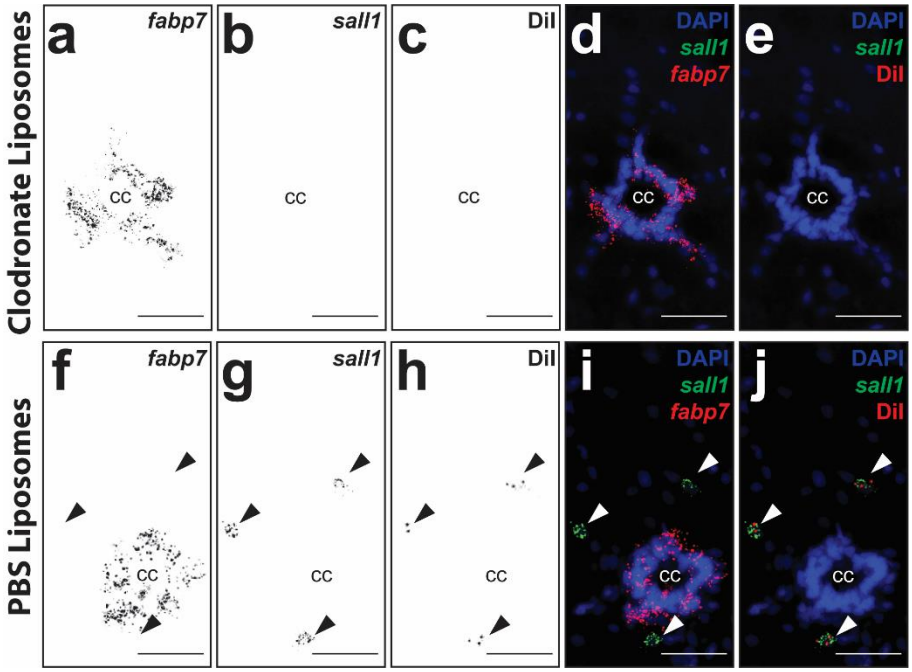

Supplementary Figure 8. Lengths and areas of tail tissues distal to amputation planes collected 14 DPA from lizards treated with clodronate or PBS liposomes. n = 10 different animals/tails for each condition. Data are presented as mean values +/− SD. Two-way ANOVA with pairwise Tukey's multiple comparison tests was used. *, $p < 0.01$ compared to corresponding PBS liposome values, respectively.

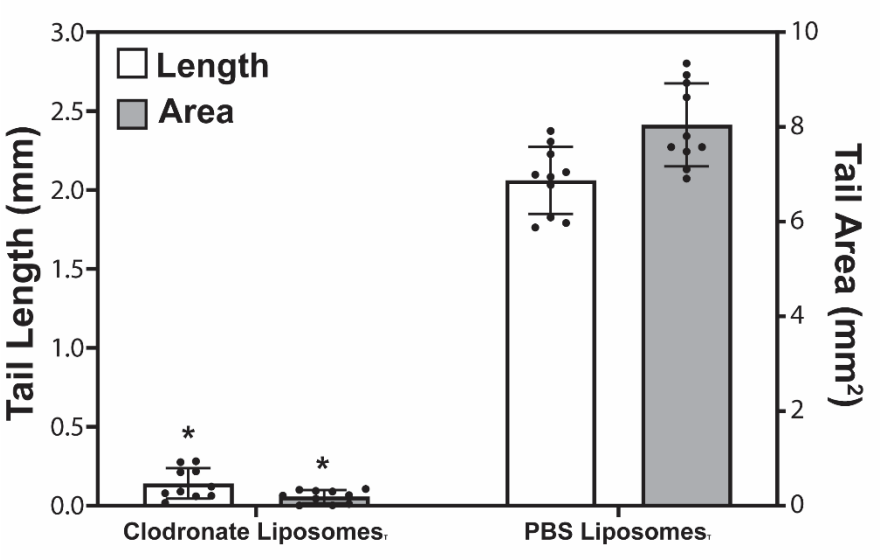

Supplementary Figure 9. Lengths and areas of tail tissues distal to amputation planes collected 21 DPA from lizards treated with vehicle control (VC), SAG, or cyclopamine (Cyc) under control, RGC depletion, or phagocyte depletion conditions. n = 10 different animals/tails for each condition. Data are presented as mean values +/− SD. Two-way ANOVA with pairwise Tukey's multiple comparison tests was used. *, #, $p < 0.01$ compared to corresponding VC length and area values, respectively, for each condition (e.g., control, RGC depletion, microglia depletion).

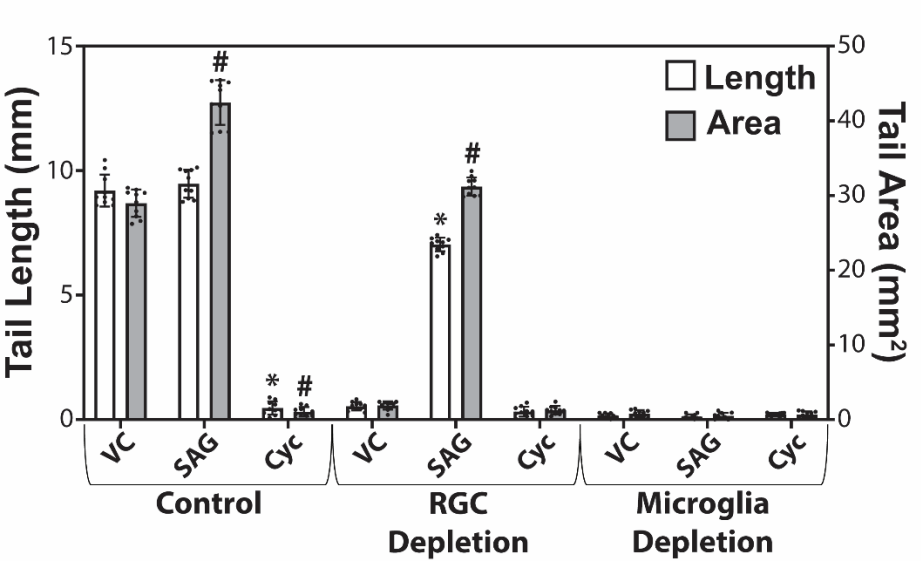

Supplementary Figure 10. (a, b) Quantified percentages of *col3a1*$^{+}$ tail fibroblasts that exhibit **(a)** EdU incorporation or **(b)** express *acta2* following treatment with vehicle control, SAG, or cyclopamine under control, RGC depletion, or phagocyte depletion conditions. n = 10 different animals/tails for each condition. Data are presented as mean values +/− SD. Two-way ANOVA with pairwise Tukey's multiple comparison tests was used. *, $p < 0.01$; ns, not significant; compared to corresponding vehicle control values for each condition (e.g., control, RGC depletion, microglia depletion).

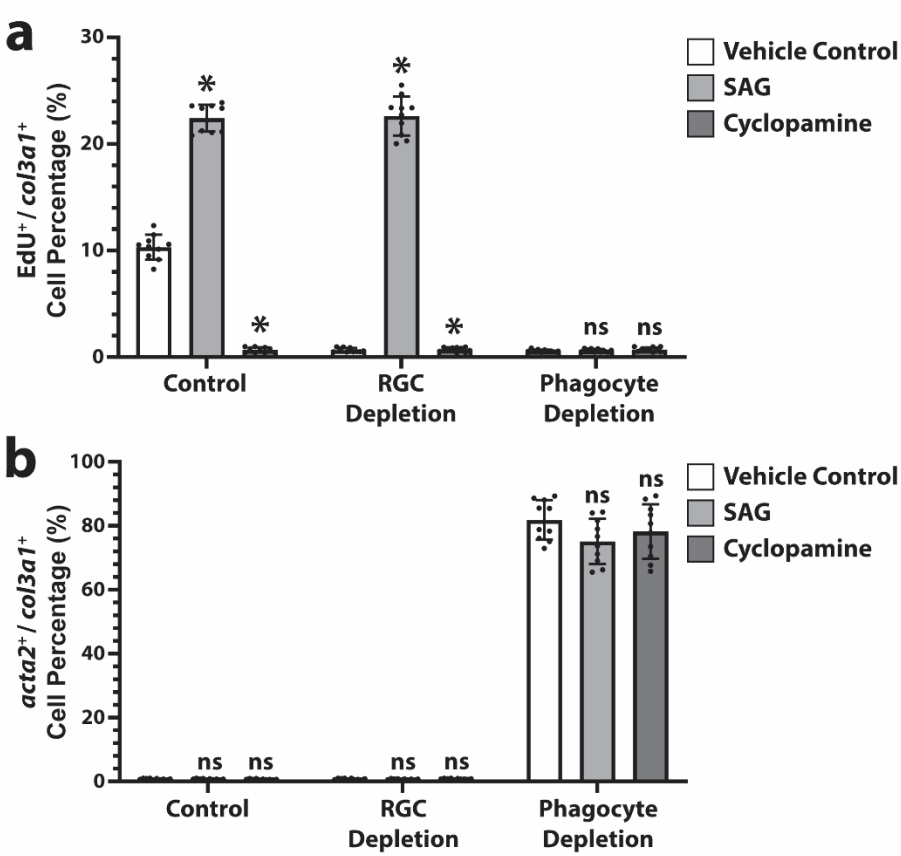

Supplementary Figure 11. Lizard limbs lack endogenous RGC and microglia populations. Quantification of (a) glial cell and (b) phagocyte densities measured in lizard tails and limbs collected 0, 7, 14, and 21 DPA. From FISH. Glial cells are subdivided into *gfap*$^{+}$ *fabp7*$^{+}$ RGCs and *gfap*$^{+}$ *fabp7*$^{-}$ "other" glial cells, such as schwann cells, and phagocytes are subdivided into *ctsk*$^{+}$ *sall1*$^{+}$ microglia and *ctsk*$^{+}$ *sall1*$^{-}$ "other" phagocytes, including macrophages and osteoclasts. n = 50 cell densities measured from five images among 10 different animals/samples for each time point. Data are presented as mean values +/− SD. Two-way ANOVA with pairwise Tukey's multiple comparison tests was used. *, $p < 0.01$.

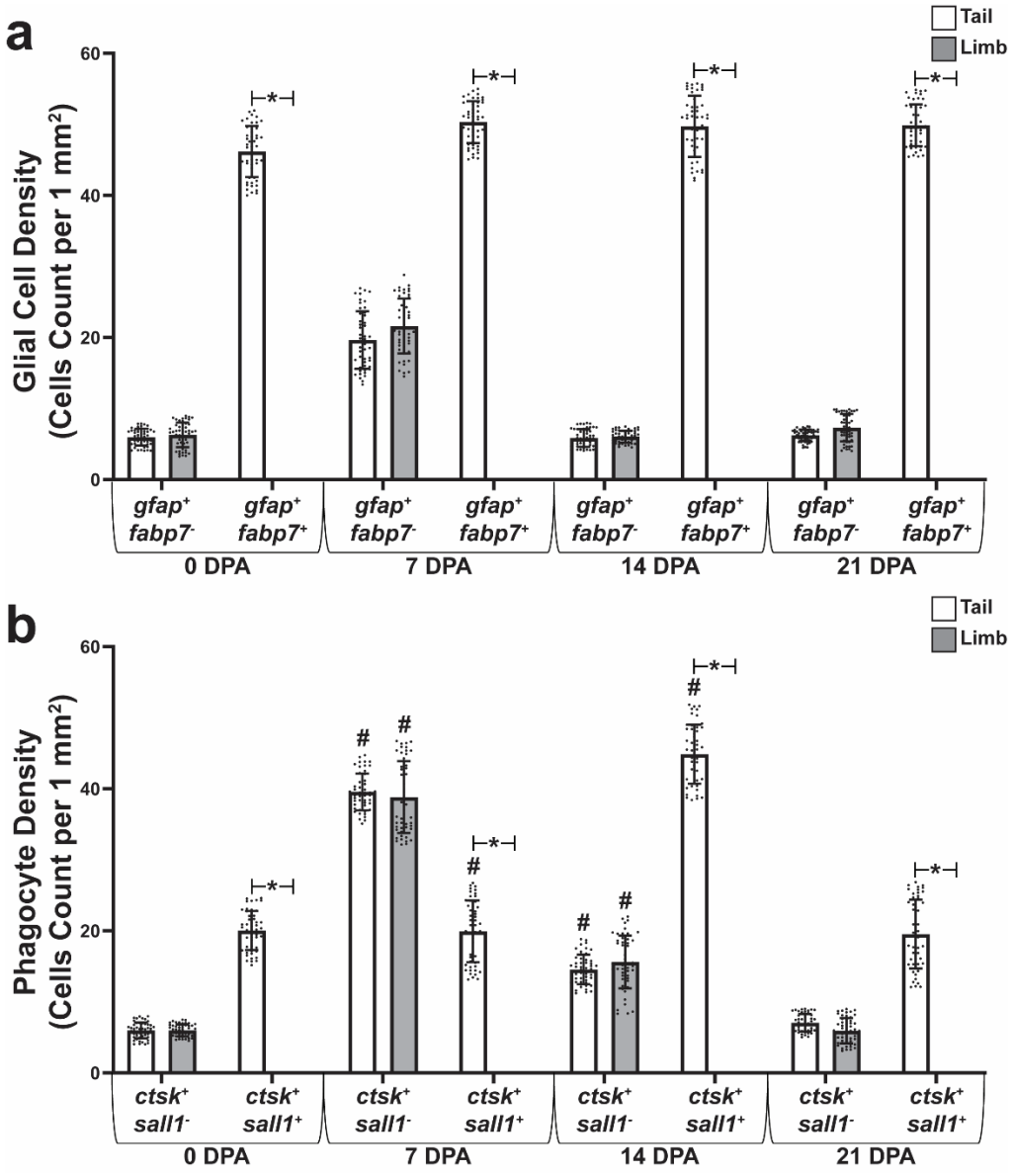

Supplementary Figure 12. Spinal cord implants induce ectopic tail-like growths on amputated lizard limbs. Lizard limbs treated with sham surgery (control) or regenerated tail spinal cord implants and analyzed by **(a, b)** gross morphologies, **(c, d)** pentachrome staining, and **(e, f)** in situ hybridization for *col2a1* and *mck* 28 DPA. While sham surgeries resulted in scar formation (a, c, e), spinal cord implants induced formation of ectopic tail-like structures that contained regenerated cartilage (d, f), muscle tissue (d, f), and regions of cell proliferation (f). eet, ectopic ependymal tube; rc, regenerated cartilage; rm, regenerated muscle.

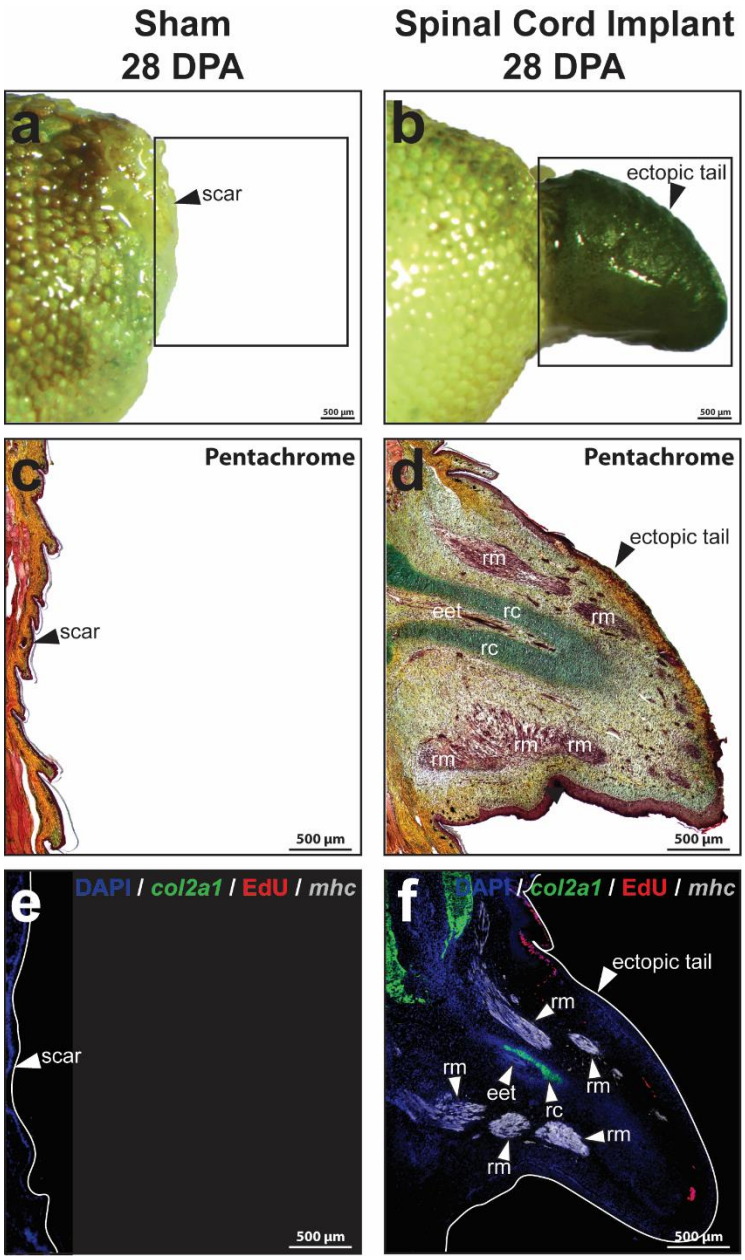

Supplementary Figure 13. RGCs and microglia of tail spinal cord pieces implanted into amputated lizard limbs contribute to regenerated structures within ectopic blastemas. (a) Experimental scheme used in ectopic blastema studies to trace RGC and microglia populations. Tail spinal cords of donor lizards were pre-transduced with AAV5(GFAPp-Cre) and AAV5(FLEX-DTR-GFP) to label RGC populations. Donor lizards were also treated DiI liposomes to label microglia. At 28 DPA, regenerated tail spinal cord pieces were collected from donor lizards and implanted into amputated limbs of untreated recipient lizards. Resultant ectopic blastemas (14 DPA) were collected and histologically analyzed for presence of labeled RGC and microglia populations within regenerated structures. **(b-d)** Representative sagittal sections of junctions between limb stumps and ectopic blastemas of recipient lizards analyzed by histology/FISH for GFP, DiI, and *fabp7* and *sall1*. Ectopic ependymal tubes continuous with spinal cord implants contained GFP$^+$ *fabp7*$^+$ RGCs and DiI$^+$ *sall1*$^+$ microglia, indicating shared origination from donor lizards. eet, ectopic ependymal tube; sci, spinal cord implant. Bar = 100 μm.

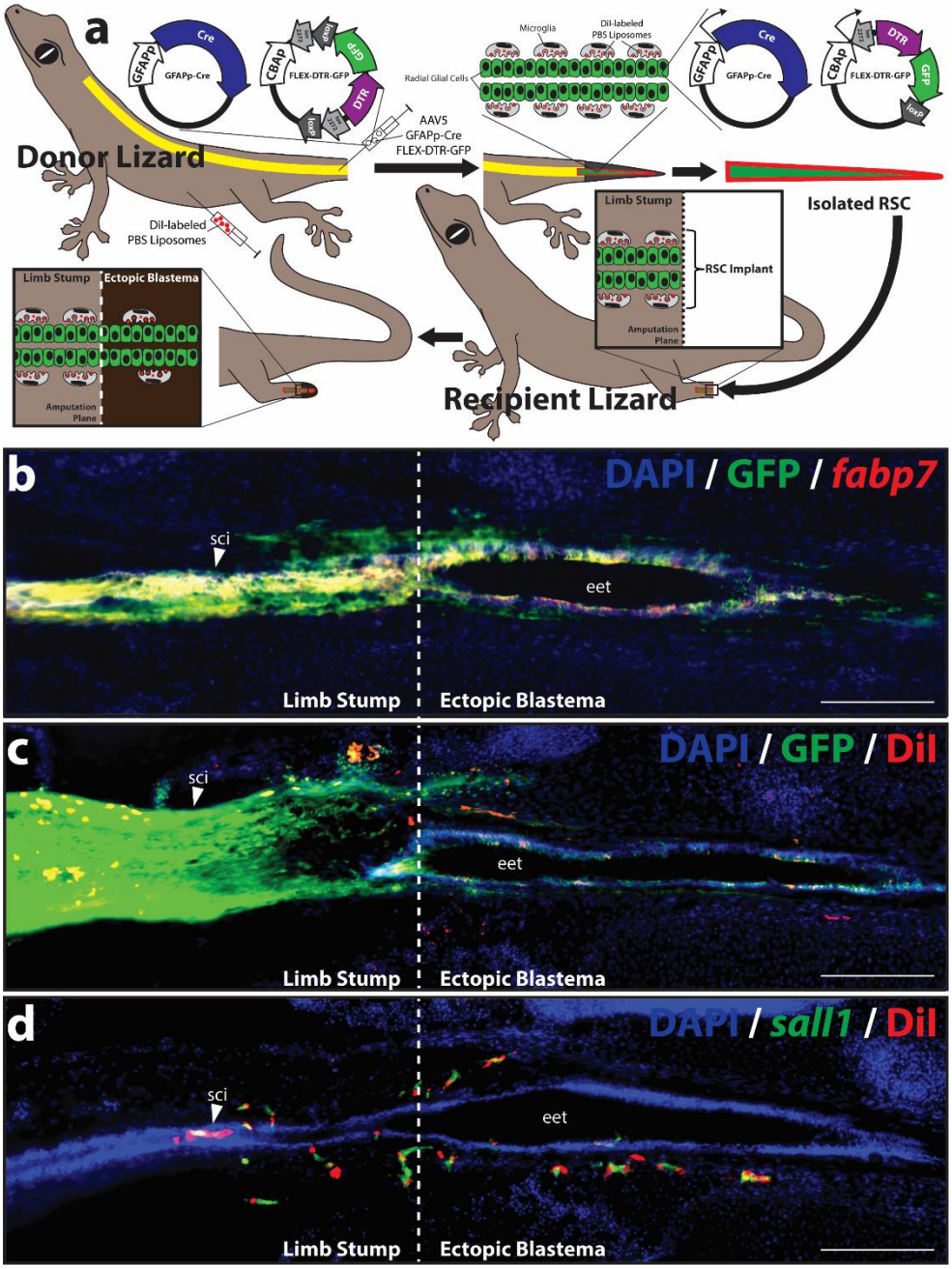

Supplementary Figure 14. Lengths and areas of limb tissue distal to amputation planes collected 14 DPA from lizards treated with sham surgery (control) or spinal cord implants. n = 10 different animals/limbs for each condition. Data are presented as mean values +/− SD. Two-way ANOVA with pairwise Tukey's multiple comparison tests was used. *, #, $p < 0.01$ compared to corresponding control length and area values, respectively.

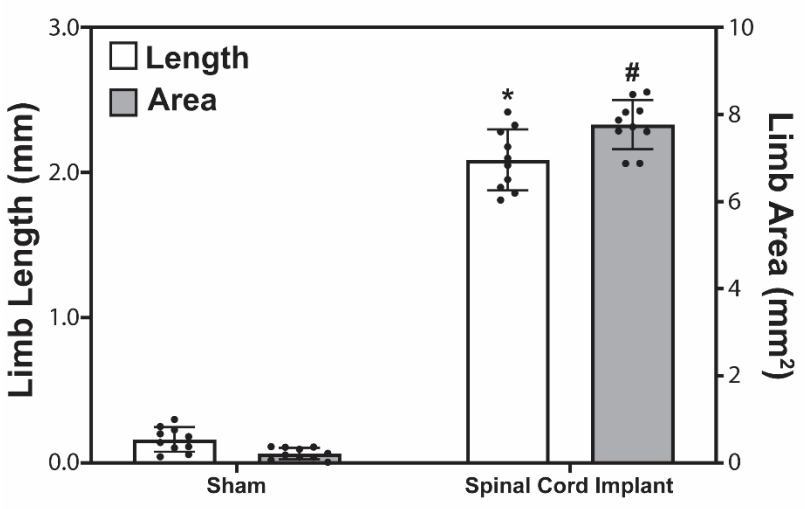

Supplementary Figure 15. Lengths and areas of tissues distal to amputation planes collected 21 DPA from lizard limbs implanted with spinal cord implants and treated with vehicle control (VC), SAG, or cyclopamine (Cyc) under control, RGC depletion, or phagocyte depletion conditions. n = 10 different animals/tails for each condition. Data are presented as mean values +/− SD. Two-way ANOVA with pairwise Tukey's multiple comparison tests was used. *, #, $p < 0.01$ compared to corresponding VC length and area values, respectively, for each condition (e.g., control, RGC depletion, microglia depletion).

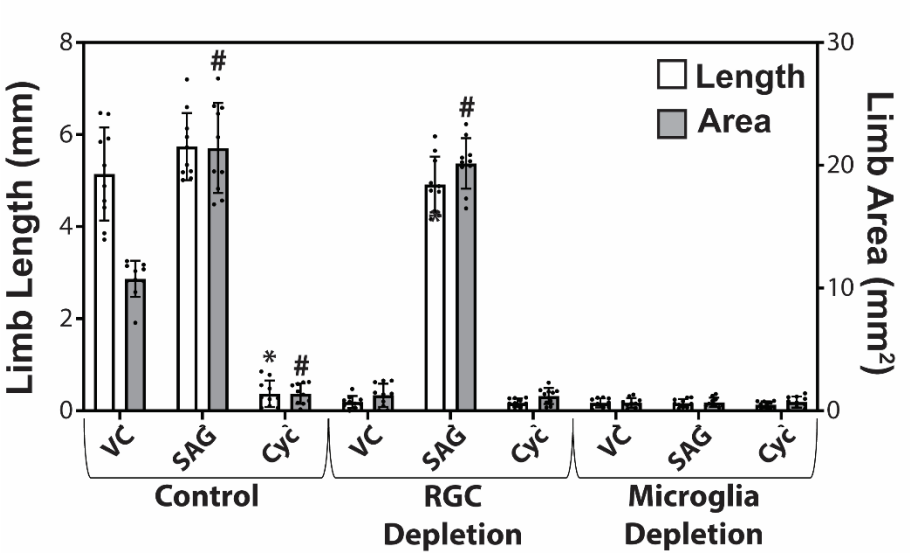

Supplementary Figure 16. (a, b) Quantified percentages of *col3a1*$^{+}$ limb fibroblasts that exhibit **(a)** EdU incorporation or **(b)** express *acta2* following implantation with intact, RGC-depleted, or microglia-depleted spinal cord implants and treatment with vehicle treatment, SAG, or cyclopamine. n = 10 different animals/tails for each condition. Data are presented as mean values +/− SD. Two-way ANOVA with pairwise Tukey's multiple comparison tests was used. *, $p < 0.01$; ns, not significant; compared to corresponding vehicle control values for each condition (e.g., control, RGC depletion, microglia depletion).

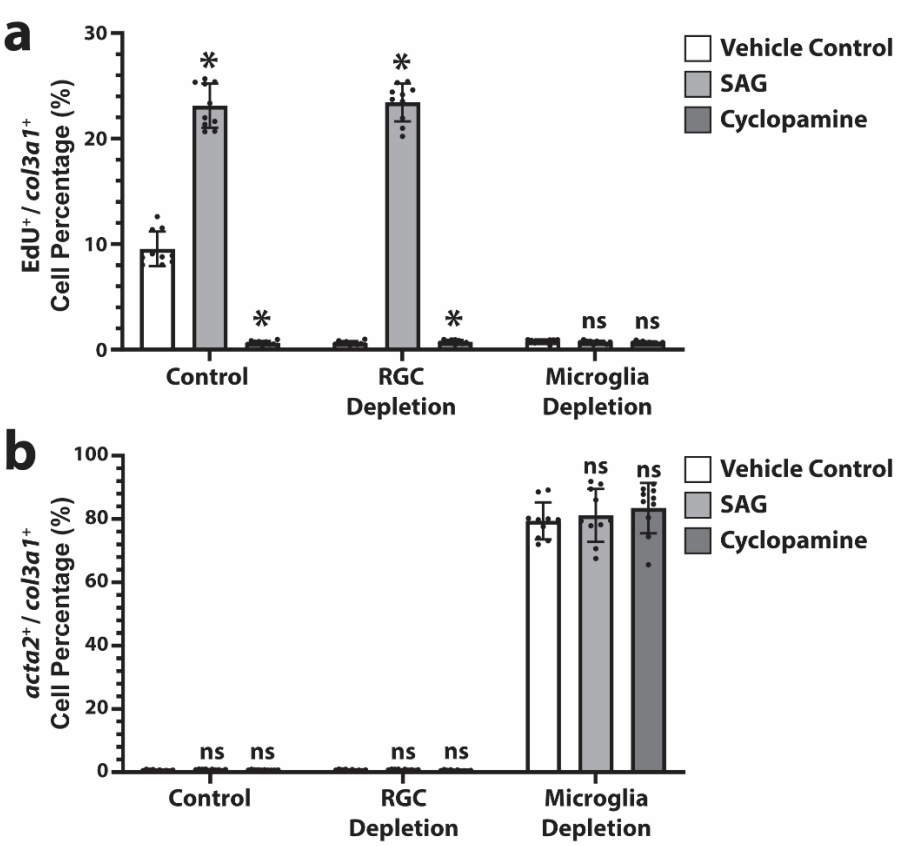

Supplementary Table 1. Catalog information for commercial probes used in FISH. All probes were custom designed by supplier Advanced Cell Diagnostics, Inc. to species-specific mRNA sequences for respective genes.

Reagent	Catalog Number
RNAscope™ Probe-Acar-acta2	1291711
RNAscope™ Probe-Acar-col2a1	882331
RNAscope™ Probe-Acar-col3a1	896371
RNAscope™ Probe-Acar-LOC100561728 (ctsk)	882321
RNAscope™ Probe-Acar-fabp7	896331
RNAscope™ Probe-Acar-LOC100562721 (mhc)	882301
RNAscope™ Probe-Acar-sall1	1058561